Металлофиз. новейшие технол. / Metallofiz. Noveishie Tekhnol.
2016, т. 38, № 10, сс. 1303–1320/ DOI: 10.15407/mfint.38.10.1303
Оттиски доступны непосредственно от издателя
Фотокопирование разрешено только
в соответствии с лицензией

ВЗАИМОДЕЙСТВИЯ ИЗЛУЧЕНИЯ И ЧАСТИЦ С КОНДЕНСИРОВАННЫМ ВЕЩЕСТВОМ

PACS numbers: 31.15.xv, 34.20.-b, 61.72.Bb, 61.72.Cc, 61.72.jd, 61.72.jj, 61.80.Az, 61.85.+p

A Study of Atomic Displacements Produced in Cascades in Irradiated α-Zr by Using Molecular Dynamics Simulations

Yu. M. Ovcharenko, S. V. Kokhan, D. O. Kharchenko, X. Wu*, B. Wen*, L. Wu*, and W. Zhang*

Institute of Applied Physics, N.A.S. of Ukraine,
58 Petropavlivska Str.,
40000 Sumy, Ukraine
**The First Institute, Nuclear Power Institute of China,*
328, the 1st Section, Changshundadao Road,
Shuangliu, Chengdu, China

We study the cascades' formation, development and annealing in pure zirconium crystals irradiated in different irradiation conditions. Statistical and geometric properties of cascades are studied in details by varying sample temperature, energy of primary knocked atoms, and direction of their motion. A possibility of channelling at cascades development is shown; it results in formation of crowdions. A change in statistical properties of the crystal during cascades' development and a relaxation time of cascades are studied. A possibility of formation of different-type defects after cascades' annealing is discussed.

Key words: molecular dynamics, embedded atom method, cascade, point defects.

У даній роботі досліджуються процеси формування каскадів, їх проходження та відпал у чистих кристалах цирконію за різних умов опромінювання. Вивчаються статистичні та геометричні властивості каскадів за різних температур, енергій первинно вибитих атомів і напрямків їх направленого руху. Показано можливість каналювання при еволюції кас-

Corresponding author: Yuriy M. Ovcharenko
E-mail: dikh@ipfcentr.sumy.ua

Please cite this article as: Yu. M. Ovcharenko, S. V. Kokhan, D. O. Kharchenko, X. Wu, B. Wen, L. Wu, and W. Zhang, A Study of Atomic Displacements Produced in Cascades in Irradiated α-Zr by Using Molecular Dynamics Simulations, *Metallofiz. Noveishie Tekhnol.*, **38**, No. 10: 1303–1320 (2016), DOI: 10.15407/mfint.38.10.1303.

кадів, що приводить до утворення краудіонів. Досліджено статистичні особливості проходження каскадів і характерний час відпалу. Проведено аналізу процесів формування структур точкових дефектів.

Ключові слова: молекулярна динаміка, метода зануреного атому, каскад, точкові дефекти.

В данной работе исследуются процессы формирования каскадов, их прохождение и отжиг в чистых кристаллах циркония при различных условиях облучения. Изучаются статистические и геометрические свойства каскадов при различных температурах, энергиях первично выбитых атомов и направлениях их движения. Показана возможность каналирования при прохождении каскадов, что приводит к образованию краудионов. Исследованы статистические особенности прохождения каскадов и характерное время отжига. Проведён анализ процессов формирования структур точечных дефектов.

Ключевые слова: молекулярная динамика, метод погруженного атома, каскад, точечные дефекты.

(Received May 25, 2016)

1. INTRODUCTION

From experimental and theoretical studies of pure metals and alloys used in atomic energy facilities, it is well known that non-equilibrium point defects produced by particle irradiation are able to manifest self-organization, where clusters of point defects emerge due to an ensemble of supersaturated non-equilibrium point defect rearrangement [1–3]. Simplest (point defects) produced by irradiation influence can form complexes of defects (bi- and three-vacancies) and complexes of interstitials. During their diffusion, they can be captured by sinks, namely dislocations, grain boundaries, voids, *etc*. Self-organization of ensemble of defects results in formation of dissipative spatial or spatial-temporal structures (clusters, voids) [4, 5]. These objects can form superlattices repeating the lattice structure of a sample [4–6]. The formation of such objects is possible in two cases: small clusters can emerge if two or more defects of one sort (vacancies or interstitials) are located at scales of several lattice constants, where their agglomeration reduces the elastic energy of the crystal; objects at the nanometre range (defect walls, voids) can be formed if the defect concentration exceeds some critical value due to point defects supersaturation. An observation of point defects' self-organization into clusters, voids, and formation of their superlattices were reported in important amount of papers devoted to experimental and theoretical studies of irradiated solids (see for example [1, 2, 7, 8] and citations therein).

During irradiation, most of non-equilibrium defects are produced,

resulting to degradation of physical and mechanical properties of the corresponding constructions. Therefore, one of the main problems in radiation material science belongs to study properties of defect microstructure formed during sustained irradiation. In general, one of low-cost and perspective approach to study radiation damages in construction materials is the multiscale modelling [9], where processes of defect formation, their dynamics, clustering and physical, and mechanical properties change due to defects rearrangement can be analysed self-consistently at different time and length scales. Among methods used in multiscale modelling, one can issue *ab-initio* calculations, molecular dynamics simulations, phase field crystals modelling, modelling spatial dynamics of point defect concentrations within the framework of the reaction rate theory, Monte Carlo simulations, and statistical mechanics computations. Multiscale modelling can predict and examine behaviour of already used structural materials by reducing time and costs compared to corresponding experimental studies, and design novel materials exploited in extreme non-equilibrium conditions. The realization of such a multiscale modelling procedure is a very ambitious problem requiring a huge database of structural element parameters, the development of corresponding computation codes cross-linked with different hierarchical levels of description, and huge computational resources. Considering some narrow problems related to study special aspects of above phenomena in most of cases, one can use a combination of few approaches of this scheme. For example, formation and dynamics of defects can be studied by combining at least several methods, namely *ab-initio* computations and molecular dynamics [10–12] or molecular dynamics and kinetic Monte Carlo simulations. Some hybrid methods such as phase-field crystal approach [13–15] can be used to describe structural disorder formation, motion of point and linear defects (dislocations), and transformations at micro- and mesoscopic scales [16–18]. As shown in Refs. [19–22], a combination of phase field theory and elasticity theory allows one to study a rearrangement of elastic stresses in the formation of defects in alloys [23]. Self-consistent approaches combining phase field theory and dislocation dynamics [24–26] was applied to explore the influence of mobile dislocations onto phase decomposition processes [27]. To study the formation of spatial-temporal structures on a surface of irradiated samples, a combination of kinetic Monte Carlo and continual approaches gives results corresponding to the experimentally observed picture of surface patterning [28, 29].

A development of methods for multi-scale modelling allows one to study specific materials used in real reactors, for example iron-based or zirconium-based alloys. Considering zirconium as a base element, one can note that zirconium as a fuel cladding material used for light and heavy water reactors is established due to combination of its prop-

erties. It has good corrosion resistance to high temperature, high-pressure water and steam, it manifests good mechanical ductility and stress, and it has low thermal neutron cross section. At the same time, it is exploited for reactor core internals such as fuel element supports, pressure tubes, core support members, and, different instrumentation assemblies. It has the following useful properties which are superior comparing to stainless steels to such as: corrosion resistance, strength under neutron bombardment, neutron economy, its use as fuel cladding elements allows one to exclude water chemistry problems, it manifests suitability for primary steam systems, it is widely used in non-nuclear applications (for example, in chemistry processing plants as chemical reactor vessels). At the same time, zirconium cannot be welded to iron, copper, or nickel based alloys due to formation of brittle intermetallics. Zirconium is characterized by low solubility of impurities like phosphorus, silicon, carbon.

As far as this material and alloys based on pure zirconium are used as a construction material in atomic energy facilities, in real situations, it usually affected by neutron and ion irradiation. Therefore, a study of cascades development in such materials is allows one to understand reason leading to physical and mechanical properties degradation under particle irradiation. From practical viewpoint, main materials are binary and ternary alloys with small concentration of alloying elements (up to two percent). Hence, the main problem in their study lies in description of defect microstructure behaviour. From the other hand, one should know properties of defect microstructure evolution in pure materials in order to compare dynamics of defects in alloys and make some recommendations for using these materials in real reactors, to extend an exploiting time of such materials.

Therefore, in this work, we focus our attention in studying defect microstructure behaviour in pure zirconium as a based element for cladding materials. The aim of the work is to study dynamics of cascade development in α-Zr crystal irradiated at different temperatures and direction of primary knocked atom with different direction of their motion. In our study, we use molecular dynamics simulation technique, where embedded atom methodology is used to describe behaviour of defect microstructure in real metallic system, namely, pure α-Zr crystal. We consider not only number of defects in cascades and a change of geometrical properties of cascade at different irradiation conditions; here, attention is also paid to study statistical properties change in irradiated crystals. We analyse defects remaining after cascade annealing.

The work is organized in the following manner. In Section 2, we discuss methodology of our simulations. Section 3 is devoted to study simulation results. Here, we initially discuss methods used to correct identification of atoms belonging to cascades. Next, we consider sta-

tistical properties of cascades, lifetime for cascades and types of defects realized after cascade annealing. Finally, we conclude in Section 4.

2. METHODOLOGY OF SIMULATION PROCEDURE

To study dynamics of atomic displacements realized in cascades in solids subjected to an irradiation influence, we will use the molecular dynamics (MD) methods, realized in programming programs package LAMMPS [30]. We perform MD simulation for pure α-Zr by using the interatomic interaction potential [31], obtained with the help of embedded atom method [32]. All calculations were done for 3*D* Zirconium crystal containing $1.8 \cdot 10^5$ atoms by using GPU computing, which allows us the computations accelerated by 20 times comparing to the standard CPU one.

A simulation procedure corresponds to numerical solutions of classical Newton equations,

$$m_i \frac{d^2 \mathbf{r}_i}{dt^2} = \mathbf{F}_i^{\text{ext}} - \frac{\partial U_i}{d\mathbf{r}_i},$$

for each of $1.8 \cdot 10^5$ atoms. Here, $\mathbf{F}_i^{\text{ext}}$ is the vector of all equilibrated forces related to potential energy of i-th atom defined by the radius vector $\mathbf{r}_i$ and the mass m_i.

All calculations were performed according to the potential No. 3 for pure α-Zr taken from the work [31], where embedded atom method was exploited [32]. A choice for the interaction potential No. 3 is stipulated by following criteria, which are made to study cascades' dynamics. It gives correct results comparing to experimental study of crystal lattice behaviour of α-Zr at elevated temperatures and corresponds good to define defects formation energies at irradiation influence. According to the embedded atom method, for the interatomic potential energy, one has $U_i = F_\alpha(\sum_{i \neq j} \rho(\mathbf{r}_{ij})) + (1/2)\sum_{i \neq j} \varphi_{\alpha\beta}(\mathbf{r}_{ij})$, where $\mathbf{r}_{ij}$ is a radius-vector between two i-th and j-th atoms, $\varphi_{\alpha\beta}$ is an interaction function of pairwise distance, ρ is a contribution related to electronic charge density acting from j-th atom onto i-th atom, F_α is an 'embedding' function related to energy needed to put i-th atom into the electronic cloud.

In MD simulation procedure, there are several limitations, approximations and parameters, which define accuracy of obtained results. Among them, the most important ones are interatomic interaction potential, simulation time-step, total simulation time, initial conditions, etc. Hence, the first important task in MD simulations is to prepare a model system for further study.

In Table 1, we collect the main parameters used for simulations of

TABLE 1. The main parameters for cascades modelling in α-Zr crystal.

Parameter	Value
Simulation box size, nm	16.31×16.95×15.98
Number of atoms N	$1.8 \cdot 10^5$
Crystal temperature T, K	300, 400, 500
Primary knock-on atom (PKA) energy E_{PKA}, keV	2, 6, 10
PKA moving direction	<0001>, $< 01\bar{1}0 >$
Thermostat parameter $\tilde{\tau}$, ps	0.2
Time step Δt, fs	0.1–1
Total time of simulation t, ps	610

atomic displacements in cascades and to study defect structure evolution in α-Zr crystal subjected to irradiation influence.

In cascades study, it is important that the maximal size of cascade should be less than the size of the studied crystals. Hence, the linear size of the model can be varied with a change in the energy of bombarding particle, affected the maximal size of cascade. The most important parameters for our MD simulations are the thermostat parameter $\tilde{\tau} = 0.2$ ps and the simulation time-step $\Delta t = (0.1-1)$ fs. The thermostat parameter $\tilde{\tau}$ is the mean time when energy exchanges between the system and the thermostat are realized. As far as energy in the crystal passed from atom to atom, therefore, the mean time for an energy exchange between two atoms or between atom and thermostat is defined by the mean period of atom oscillations. Hence, the quantity $\tilde{\tau}$ is the mean period of atom oscillations in a crystal. The simulation time-step Δt should be much more less than the quantity $\tilde{\tau}$ for detailed study of atoms' positions.

In our computing, we use two values for simulation time step. The minimal one was chosen as $\tilde{\tau}/2000$, that gives $\Delta t = 0.1$ fs. This value was used at that time, when cascade of atomic displacements occurs and large number of atoms attains large values of kinetic energy comparing to atoms, which do not take part in cascade. The maximal value for the simulation time-step was fixed as $\Delta t = 1$ fs ($\tilde{\tau}/200$). It was used for simulations before cascade appearance and after its relaxation.

The value of $\tilde{\tau}$ can be obtained in the framework of harmonic approximation in the following way. It is known that atoms of the crystal oscillate with a frequency ω ranging from zero up to the Debye frequency ω_D. The corresponding distribution function $g(\omega)$ over oscillating frequencies obeys the relation [33]:

$$g(\omega) = 9N\omega^2/\omega_D^3. \quad (1)$$

Rewriting Eq. (1), one can obtain the distribution function over oscillation period τ as follows:

$$g(T) = \frac{72N\pi^3}{\omega_D^3 \tau^4}. \quad (2)$$

By taking into account that the total number of elastic waves generated by atoms in the crystal is equal to $3N$, one can write a formula for the mean period of atomic oscillations:

$$\tilde{\tau} = \int_{2\pi/\omega_D}^{\infty} \frac{24\pi^3 d\tau}{\omega_D^3 \tau^3} = \frac{3\pi}{\omega_D}. \quad (3)$$

By using the experimental data for the Debye temperature, $T_D = 291$ K, for pure α-Zr and the relation $\omega_D = kT_D / \hbar$, where k, $\hbar$ are the Boltzmann and Dirac constants, respectively, one finds the mean period of atomic oscillations, $\tilde{\tau} = 0.2$ ps.

3. RESULTS AND DISCUSSIONS

3.1. Cascade Domains Identification Procedure

During cascades formation and their evolution, domains of structural disorder are formed, where crystalline lattice is broken totally. Here, most of atoms attain kinetic or potential energy, which differs essentially from that out of cascade. It allows one to distinguish cascade domain in a crystal according to values of kinetic and potential energies of atoms. However, this procedure of cascade identification cannot give the total information about the size of the cascade domains and the number of atoms in cascades with good accuracy. Indeed, a finite number of atoms belonging to the structural disorder configuration due to their chaotic location can have both kinetic and potential energies of the same values that outside cascade atoms have. Therefore, this procedure should generalize by considering structural configurations of atoms in the crystal during the cascade development.

In our simulations, we initially prepare the sample of α-Zr at fixed temperature with ideal structure configuration. To distinguish atoms belonging to cascade and atoms of a bulk α-phase, the Common Neighbour Analysis (CNA) was exploited [34–36]. According to this approach, two nearest neighbour atoms assumed to be bounded if the distance between them does not exceed the cutting radius r_{cut}. Its value should lie in the interval between two peaks in a radial distribution function of atomic positions [37]. Obviously, a suitable choice of values of r_{cut} is the mean value between distance between selected atom to it nearest neighbours and a distance between selected atom and next

nearest neighbours. According to this scheme, one can choose a value for the cutting radius for different type of crystalline lattices.

In Figure 1, we plot graphical explanation of cascade identification by using values of kinetic and potential energies and the CNA method. The PKA energy was taken $E_{\text{PKA}} = 10$ keV at temperature $T = 300$ K; PKA direction is <0001>; the time for the cascade development is $t = 5.4$ ps.

By comparing energy difference of all atoms (see Fig. 1, *a*), one finds that only $N_{\text{C}} = 8314$ number of atoms of the crystal can be distinguished as atoms belonging to the cascade. The cascade surface and volume of the cascade are $S_{\text{C}} = 4311.88$ nm^2 and $V_{\text{C}} = 23282.1$ nm^3. By using the CNA method, we can mark atoms by phase compound difference, which belong to the cascade with h.c.p. symmetry breaking (see Fig. 1, *b*). Indeed, it becomes possible as far as at initial stage (before cascade formation) all atoms obey h.c.p. symmetry. In this case, one gets the following information: the number of atoms having h.c.p. symmetry breaking is $N_{\text{C}} = 15292$, whereas the cascade surface and its volume take values $S_{\text{C}} = 4808.40$ nm^2 and $V_{\text{C}} = 35378.2$ nm^3, respectively. Here, we need to stress that the CNA method cannot give total information about cascade properties, if it is used separately. Indeed, due to chaotic atomic mixing in cascades, some atoms can randomly have configuration of nearest neighbours allowing one to identify them as atoms with h.c.p. symmetry. In such a case, the CAN method fails, and these atoms with randomly formed h.c.p. configuration can be identified as atoms out of cascades. In other time step, microstructure of cascade is changed, some other atoms in cascade can be characterized randomly by the h.c.p. symmetry, and as a result, the CAN

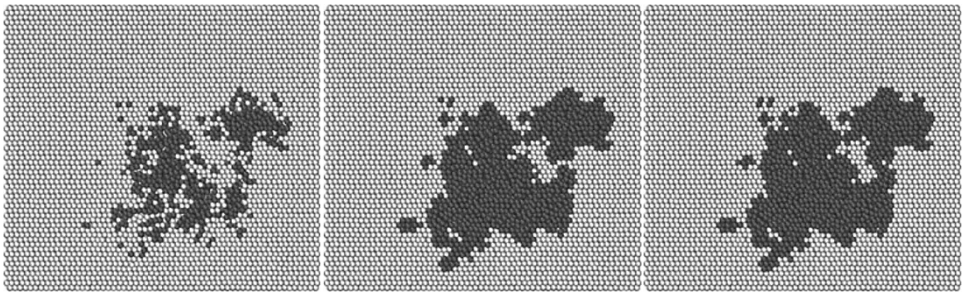

Fig. 1. The cascade identification in α-Zr crystal with $N = 180000$ atoms by analysing energy of atoms and atom neighbour positions (phase compound) at $T = 300$ K, $E_{\text{PKA}} = 10$ keV, PKA direction is <0001> at time $t = 5.4$ ps (cross-section of the crystal with a cascade): identification by energy only (*a*); identification by phase compound only (*b*); identification by energy and phase compound (*c*).

method can fail in this way. To avoid such ambiguity, we propose to combine above two methods for correct identification of atoms in cascades. Therefore, next, we consider phase compound of atoms by using the CAN method and analyse difference in kinetic and potential energies of all atoms in the system. The corresponding illustration of such combined approach application is shown in Fig. 1, *c*. Here, we get the correct number of atoms in cascade $N_C = 15763$, surface and volume of excited ensemble of atoms $S_C = 4792.53$ nm^2, $V_C = 36407.8$ nm^3, considered below as real cascade.

The corresponding analysis of volume and surface of all studied cascades of their evolution allows us to conclude that all atoms inside the disturbed ensemble are identified as atoms belonging to cascades. Therefore, the proposed combined approach can be used well to study properties of cascades in h.c.p. crystals. It can be developed to study cascades formation and their evolution in metals and alloys with other symmetries.

3.2. Statistical Characteristics of Cascades

By using above generalized approach for cascades identification, we studied dynamics of the number of atoms in cascades, cascade surface and volume, respectively, by changing energy of PKA and the temperature of the crystalline system. In our study, we have considered changes in of internal energy, volume and density of irradiated samples.

In Figure 2, snapshots are shown for different stages of one cascade formation, its evolution and annealing in pure α-Zr, where the temperature of unirradiated sample was chosen as $T = 300$ K, the energy for PKA we set $E_{PKA} = 10$ keV, PKA moves in the direction <0001> (see Fig. 2, *a*). According to obtained results, one finds that, during time interval $t \simeq 0.5$ ps , the cascade attains it maximal size (cf. Figs. 2, *b*, *c*) related to a thermal spike. After this stage, the annealing of cascade is realized.

Let us consider stages of cascade development in detail. At initial stages of cascade formation when energy of knocked atoms takes extremely large values comparing to other atoms of the crystal, channelling processes can be realized. It is well seen in Fig. 2, *a* (thin part of the cascade). In order to explain possibility of channelling, we have considered trajectories of particles responsible for cascade development. The corresponding atomic configuration and trajectories of atoms at initial stages of cascade formation are shown in Figs. 3, *a*, *b*. It is well seen that, along indicated direction of motion of PKA, it moves along the line. The channelling distance of PKA is $\lambda_C = 11$ nm. In time instants when cascade attains maximal size (thermal spike), one can observe one-dimensional thickening of atoms meaning formation of

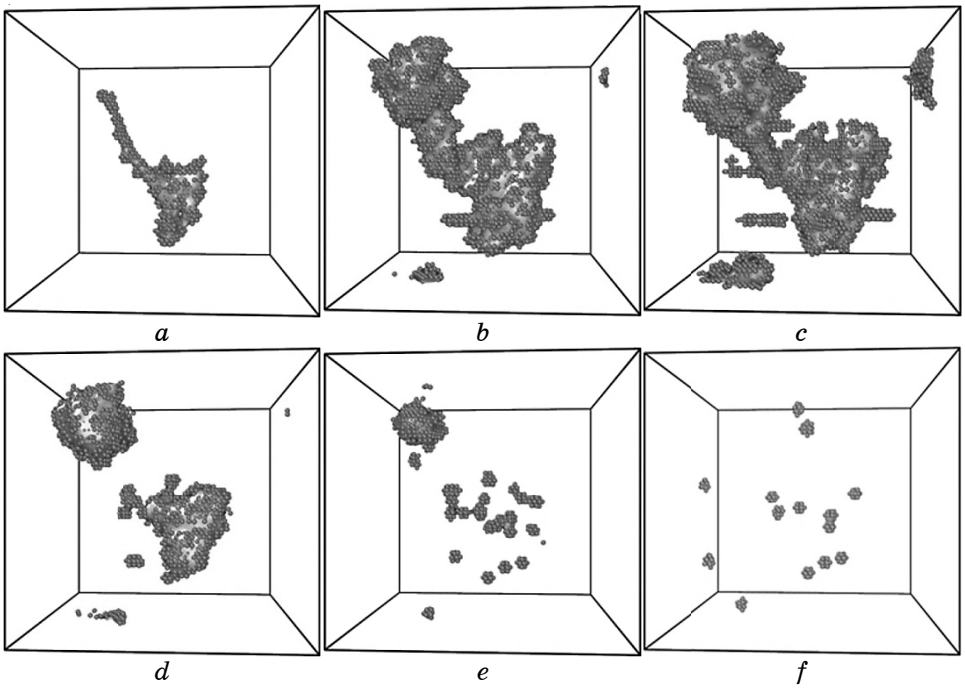

Fig. 2. Snapshots of evolution of cascade development in crystal of α-Zr containing $N = 180000$ atoms at $T = 300$ K, and PKA energy $E_{PKA} = 10$ keV: $t = 0.1$ ps (*a*), $t = 0.3$ ps (*b*), $t = 0.5$ ps (*c*), $t = 3.3$ ps (*d*), $t = 5.3$ ps (*e*), $t = 605$ ps (*f*).

crowdions (see Figs. 3, *c*, *d*). For these cascade domains, no channelling processes were observed (see Fig. 3, *d*). At the same time, some straight-line thickening is realized (see Fig. 3, *c*).

In Figures 2, *b*–*d* on low and rights sides of modelling domains, fragments of cascades are shown due to periodic boundary conditions. It is well seen that the cascade domain is broken into separated initially large domains (Figs. 2, *b*, *c*). During annealing, it breaks into small domains, where only small number of defects remains in the system (Fig. 2, *d*).

To make a quantitative description of cascades' evolution, we calculate time dependences for internal energy E, volume V, and density of the sample during cascade development and annealing (see Figs. 4, *a*, *c*, *e*). Time dependences for cascade volume V_C, its surface S_C, and number of atoms N_C in cascade are obtained for domains where h.c.p. symmetry breaking emerge (see Figs. 4, *b*, *d*, *f*). Simulations were provided at temperatures $T = 300$, 400, 500 K and different PKA energies: $E_{PKA} = 2$, 6, 10 keV. Initial directions for PKA atom motion were chosen (<0001>, $< 01\bar{1}0 >$) for each PKA energy value and for each temperature. Statistical characteristics of cascades are qualitatively same

at fixed PKA energy and temperature independently on the direction of PKA atom motion. Next, we consider their quantitative differences in details.

We summarize calculated values for maximal cascade volume $V_C^{(max)}$, cascade surface $S_C^{(max)}$ and number of atoms in cascades $N_C^{(max)}$ in α-Zr crystals at different vales of PKA energy and different direction of PKA motions at 300, 400, 500 K in the Table 2.

According to our analysis of obtained data, we have found that at temperatures of the sample 400 K and 500 K all cascades with PKA direction <0001> are characterized by larger sizes comparing to cascades simulated at the same other parameters with PKA direction $< 01\bar{1}0 >$. We have found that cascade sizes are increases with an increase in the irradiation sample temperature independently on the PKA directions. It means that, at elevated temperatures of irradiated

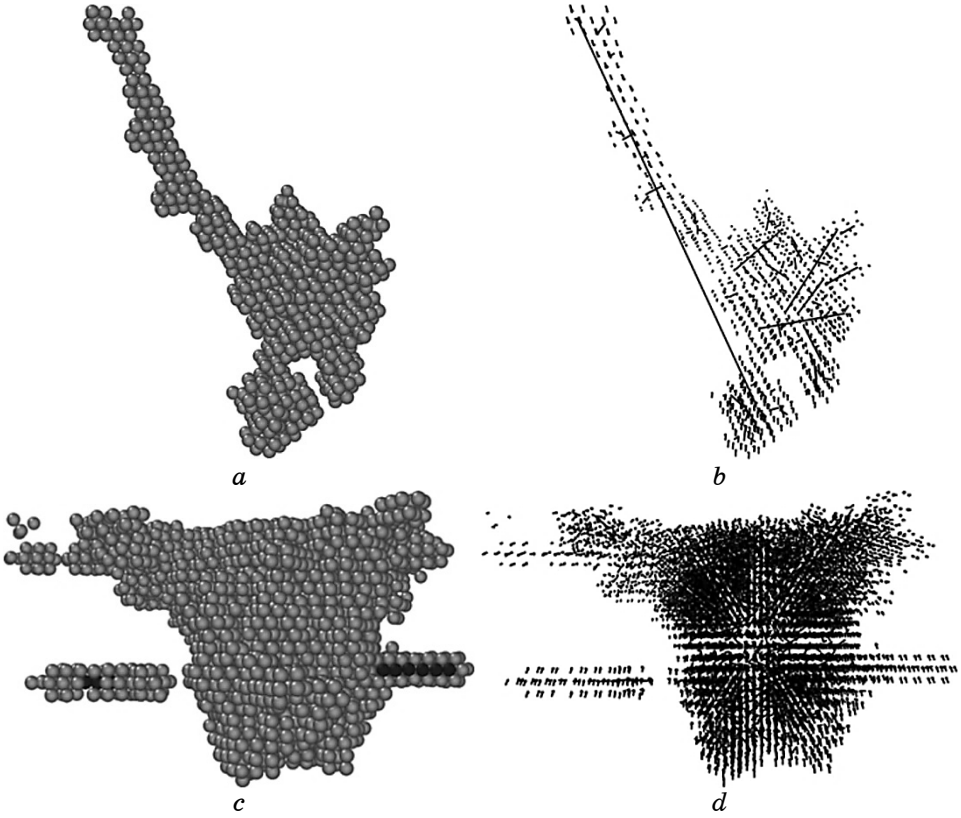

Fig. 3. Channelling and crowdion formation in crystal α-Zr during cascade development: perturbations of atoms at channelling (*a*), trajectories of atoms in cascade at channelling (*b*), perturbation of atoms at crowdions formation (*c*), trajectories of atoms at crowdions formation (*d*).

sample, irradiation damages will grow. Illustrations for cascades at their maximal sizes allow one to see crowdions formation as was shown in Fig. 3, *c*.

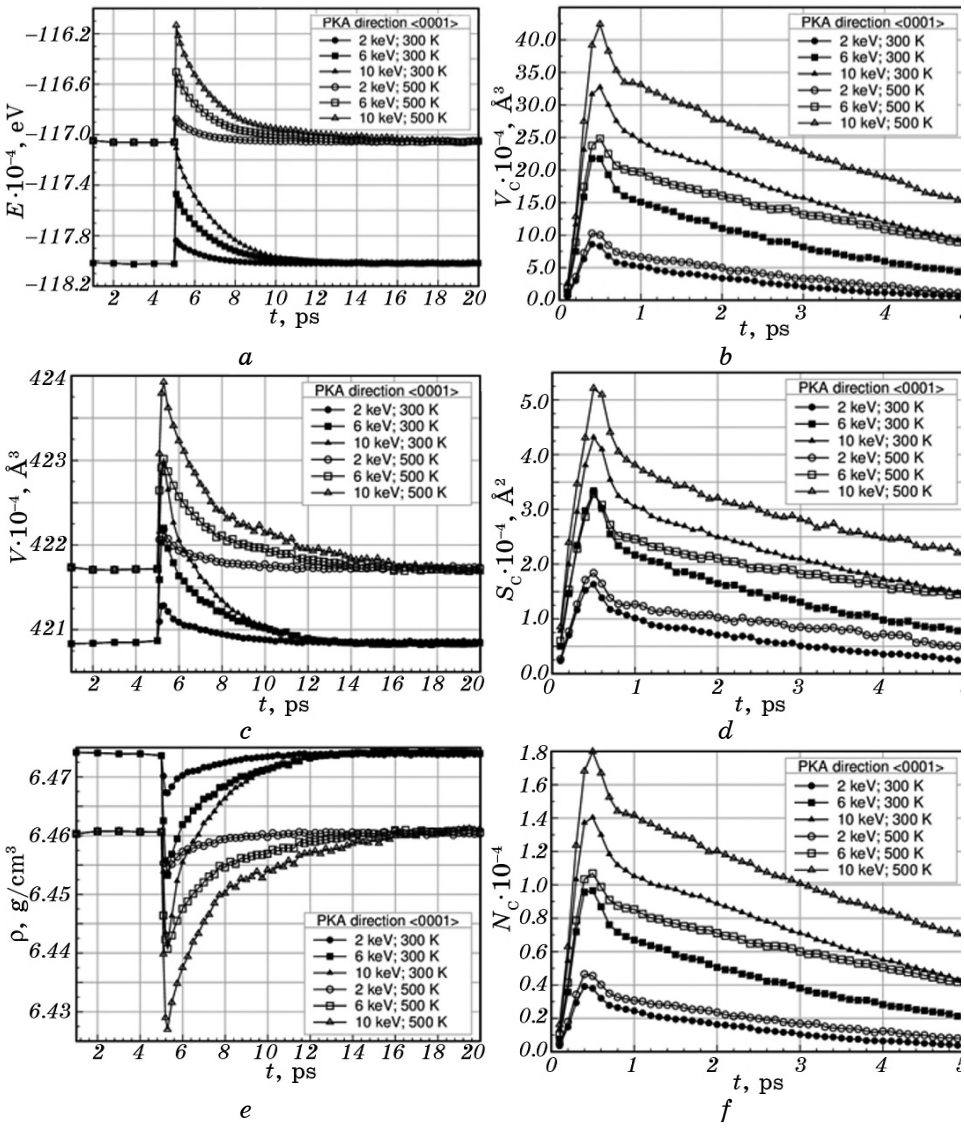

Fig. 4. Time dependences of statistical parameters of cascades at temperatures 300 K and 500 K; PKA direction is <0001>. Panels *a*–*f* correspond to dynamics of internal energy, cascade volume, volume of the sample, cascade surface, density of the sample, and number of atoms in cascade, respectively.

TABLE 2. Maximal values of cascade volume $V_C^{(max)}$, its surface $S_C^{(max)}$, and number of atoms in cascade $N_C^{(max)}$ in α-Zr sample at different values of PKA energy, direction of PKA motion and temperature of the sample.

	E_{PKA}, keV	2		6		10	
	Direction	<0001>	< 01$\bar{1}$0 >	<0001>	< 01$\bar{1}$0 >	<0001>	< 01$\bar{1}$0 >
T = 300 K	$V_C^{(max)}$, nm^3	8212.26	9104.83	20878.50	21363.80	32161.60	33418.70
	$S_C^{(max)}$, nm^2	1324.24	1730.95	2709.99	3235.76	4318.11	4374.50
	$N_C^{(max)}$	3629	4126	9090	9436	13897	14422
	Cascade form	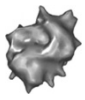	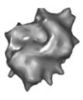	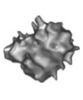	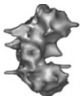		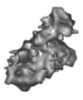
T = 400 K	$V_C^{(max)}$, nm^3	9259.53	9195.95	24741.00	24449.10	37117.80	32880.60
	$S_C^{(max)}$, nm^2	1557,20	1470.88	3626.45	3821.14	5230.81	4181.34
	$N_C^{(max)}$	4163	4022	10700	10759	16216	14367
	Cascade form						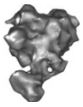
T = 500 K	$V_C^{(max)}$, nm^3	9402.16	8659.34	25781.10	25651.60	41374.00	37973.80
	$S_C^{(max)}$, nm^2	1743.58	1276.91	3809.81	3503.99	5175.19	4685.57
	$N_C^{(max)}$	4255	3838	11122	10984	17551	16179
	Cascade form						

3.3. Determination of Cascades Lifetime

One of the important quantities in studying cascade dynamics is the relaxation time of cascades τ_C (lifetime of cascade). To define this quantity, one should consider dynamics of the kinetic and potential energy of the system during cascade evolution. Indeed, as far as, even at large values of the energy of PKA, the cascade will have macroscopic size, one can expect that, in a massive sample, a temperature of cascade will tend to the temperature of the sample very fast, whereas crystal will have unrelaxed (unannealed) defect structure characterized by large amount of metastable non-equilibrium defects. By assuming the temperature as a quantity related to kinetic energy of all atoms of the crystal, one can consider dynamics of the corresponding kinetic and potential energies to define cascade lifetime τ_C.

According to protocols for kinetic and potential energies shown in Figs. 5, *a*, *b*, one finds that, even at time interval of 10 ps, the temperature (kinetic energy) of the crystal takes values of that before atomic

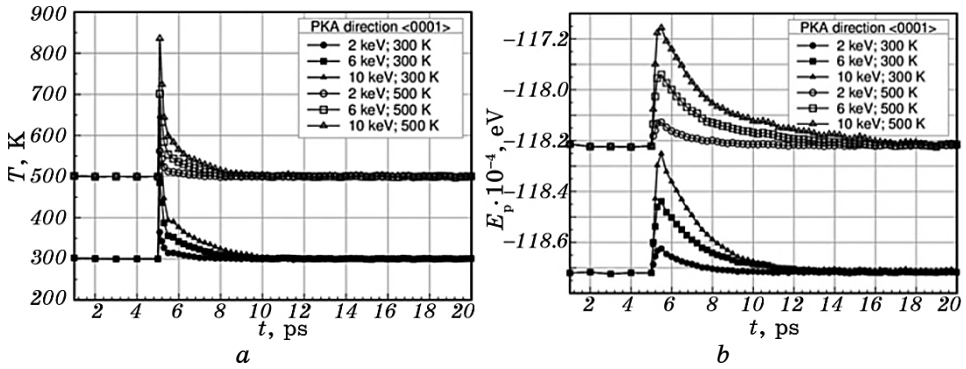

Fig. 5. Protocols for temperature (kinetic energy) T and potential energy E_p of the sample.

collisions (around initial temperature). As far as crystal after this time interval is characterized by large amount of non-equilibrium defects, which are able to diffuse along the crystal, the potential energy will change slowly comparing to kinetic energy. Therefore, to calculate cascade lifetime, one can study dynamics of potential energy as most appropriate quantity to measure lifetime for non-equilibrium (metastable) defect structure in the sample.

To determine cascade lifetime τ_C, one can use protocols for the number of defects in cascade from one hand and a relaxation time for potential energy. Here, we have restriction related to determination of the number of atoms in cascades. The number of defects in cascade is determined by very complicated procedure by taking into account two criteria related to energy difference of atoms in the sample and the CNA method. Therefore, one can use the simplest way to define cascade lifetime as a time when the potential energy E_p of the sample decreases in $e \simeq 2.71$ times. Here, we do not need to take care about configurations of nearest neighbours of selected atom, all needed information about ensemble of non-equilibrium defects can be found in protocols for potential energy of the crystal. To approximate obtained data in protocols for E_p, we use standard exponential decaying fitting, $E_p = E_{p0} + E_{pd} \exp(-t / \tau_C)$, where E_{p0} is the potential energy before cascade formation; E_{pd} is the energy contribution responsible for nonequilibrium defects formation.

In Table 3, calculated values of cascade lifetime τ_C depending on PKA energy E_{PKA} and PKA direction are shown at different temperatures.

It is logically explained that cascade lifetime τ_C will increase with growth in PKA energy E_{PKA} at fixed temperature. Indeed, the larger energy of PKA the larger will be cascade size. Therefore, the formed crowdions, which will move from the centre of the cascade, will be sep-

TABLE 3. Relaxation time for cascades in α-Zr crystal.

E_{PKA}, keV	2		6		10	
PKA direction	<0001>	$< 01\bar{1}0 >$	<0001>	$< 01\bar{1}0 >$	<0001>	$< 01\bar{1}0 >$
$\tau_C^{(300\ K)}$, ps	1.63	1.19	2.13	2.09	2.33	2.22
$\tau_C^{(400\ K)}$, ps	1.43	1.39	1.96	1.85	2.35	2.34
$\tau_C^{(500\ K)}$, ps	1.35	2.32	2.19	2.44	2.65	2.85

arated at elevated distances. As usual, crowdions are related to interstitials. Hence, after very short time interval of cascade annealing, one can observe separated interstitials in the crystal. As far as initially, the studied sample had ideal crystalline structure, therefore, the number of formed interstitials after cascade thermal spike should correspond to the number of vacancies. If we increase the energy of PKA, then, the number of such point defects (Frenkel pairs) will grow and domain size of cascade development will increase. It means that the crystalline system should have much more time for relaxation related to recombination of vacancies and interstitials for large cascades.

Comparing data related to different irradiation temperatures, one finds that initial temperature of the sample does not affect onto cascade life-time at low PKA energies ($E_{PKA} = 2$ keV, 6 keV); whereas, at elevated PKA energy ($E_{PKA} = 10$ keV), the life time increases with the sample temperature increase. Comparing data for τ_C for different PKA directions at the same values of PKA energy and temperature, one finds that the life time is lower if the $< 01\bar{1}0 >$ PKA direction is chosen comparing to PKA direction <0001> at low temperatures of the sample.

3.4. Type of Defects after Cascade Relaxation

During cascades annealing, a large amount of point defects remains in a crystal comparing to their equilibrium values. These defects lead to an emergence of uncompensated stresses in a crystal that increases total energy of the crystalline system. To compensate such stresses and to reduce the energy of the system, point defects are arranged into clusters and, therefore, from energetic viewpoint, a cluster of defects is more energetically favourable than dissolution of separated non-equilibrium defects in a bulk. In our simulations in α-Zr crystals, it was found that special type of defects can emerge, where some of them can be considered as stable and some are metastable ones (see Fig. 6). Here, one can observe separated interstitials (se Fig. 6, *a*) and interstitials in a form of a dumbbell (two nearest interstitials are located be-

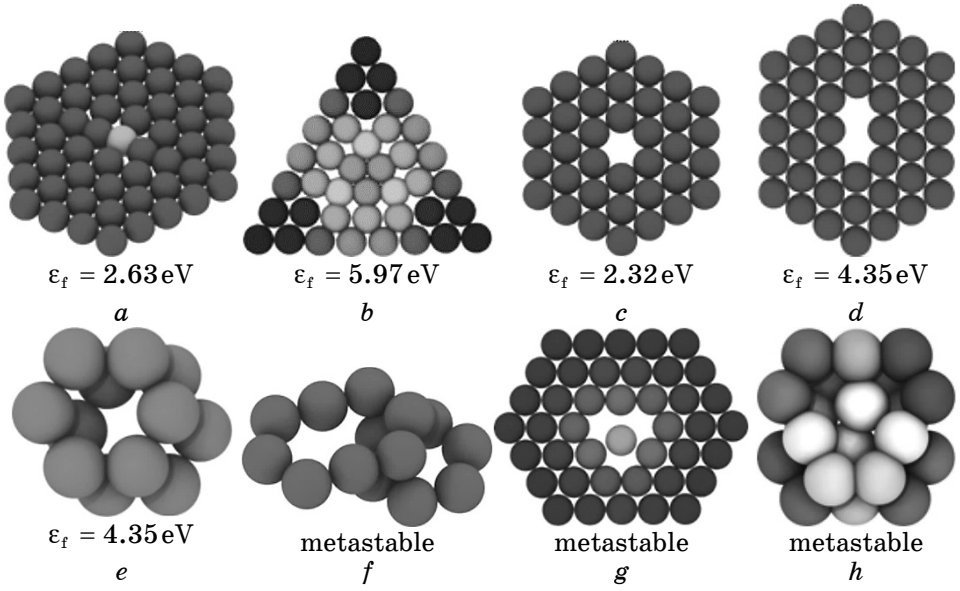

Fig. 6. Types of defects, their formation energy ε_f, and defects' life-time τ emergent after cascade annealing at short time scales: single interstitial (*a*), three-interstitial cluster (*b*), single vacancy (*c*), bi-vacancy cluster (*d*), bi-vacancy cluster with vacancies located in nearest atomic planes (*e*), three-vacancy cluster (two vacancies are in the same plane and one vacancy in nearest plane) (*f*), three-vacancy with one interstitial (metastable object) (*g*), vacancy cluster containing six vacancies and two interstitials (metastable object) (*h*).

tween nearest atomic planes) [38], clusters of interstitials (three nearest interstitials shown in Fig. 6, *b*), single vacancy, bi-vacancy clusters, and three-vacancy clusters (see Figs 6, *c*, *d*, *e*, *f*), and vacancy clusters with more than three vacancies (see Figs. 6, *g*, *h*).

We identify positions of such defects by using potential energy values of atoms and centrosymmetry parameter (*CSP*) defined as follows:

$$CSP = \sum_{i=1}^{N_V/2} \left| \mathbf{r}_i + \mathbf{r}_{i+N/2} \right|^2, \tag{3}$$

where $\mathbf{r}_i$ and $\mathbf{r}_{i+N/2}$ are radius-vectors for spatial coordinates computed from a marked central atom toward pair of diametrically opposite neighbour atoms with respect to central one, N_V is a coordination number for the crystal (for pure α-Zr one has $N_V = 12$) [36].

To identify defects and their position, we took into account the following criteria. If there are not defects near the marked atom, then *CSP* takes values about zero. However, in the case of symmetrical location of pair of defects (see, for example, Fig. 6, *g*), *CSP* takes around

zero values. In such a case, one should analyse potential energy values (values of the potential energy of the atom in defect free zone and zone containing defects are different always). It was found that clusters of defects in Figs. 6, *b*, *d*, *e* are stable; they can change their position and diffuse, whereas clusters in in Figs. 6, *f*, *g*, *h*, are metastable; they can transformed in more stable configurations.

4. CONCLUSIONS

Molecular dynamics simulations in pure α-Zr crystals irradiated at different irradiation regimes allows us to find following regularities in defect microstructure behaviour.

At initial stages of cascades formation when kinetic energy of knocked atoms takes extremely large values comparing to that in a bulk, channelling processes are realized. These processes lead to atomic displacements far from the centre of cascades. It was shown that, at elevated energies of primary knocked atoms up to 10 keV, the channelling distance takes value around 11 nm. A time interval before thermal spike is around 0.4 ps; it does not depend on the temperature of the crystal, energy and direction of motion of primary knocked atom. It was shown that at time instants related to thermal spike emergence crowdions are formed. These objects move from the centre of cascade toward undisturbed zone of the bulk leading to formation of interstitials. Considering change of geometric properties of cascades, we have shown that the size of studied cascades (volume, number of atoms in cascades) increases with the temperature growth. By studying defect microstructure evolution at cascade annealing, it was found that the relaxation time of cascades could play a role of an effective parameter describing radiation damages at molecular dynamics simulations.

This work was financially supported by the Sichuan Province International Science and Technology Cooperation and Exchange Research Program (2016HH0014) and the China Postdoctoral Science Foundation (2015M582575).

REFERENCES

1. G. S. Was, *Fundamentals of Radiation Materials Science* (Berlin–Heidelberg: Springer-Verlag: 2007).
2. D. Walgraef, *Spatio-Temporal Pattern Formation* (New York–Berlin–Heidelberg: Springer-Verlag: 1996).
3. W. Jager, P. Ehrhart, and W. Shchilling, *Nonlinear Phenomena in Materials Science* (Eds. G. Marten and I. P. Kubin) (Aedermannsorrf, Switzerland: Trans. Tech. Publications: 1988).
4. J. H. Evans, *Nature*, **229**: 403 (1971).
5. A. Jostobns and K. Farrel, *Rad. Effects*, **15**: 217 (1972).

6. J. O. Steigler and K. Farrel, *Scr. Metall.*, **8**: 651 (1974).
7. D. Walgraef, J. Lauzeral, and N. M. Ghoniem, *Phys. Rev. B*, **53**: 14782 (1996).
8. F. Kh. Mirzoev, V. Ya. Panchenko, and L. A. Shelepin, *Physics-Uspekhi*, **39**: 1 (1996).
9. E. Weinan, *Principles of Multiscale Modeling* (Cambridge: Cambridge University Press: 2011).
10. C. Varvenne, O. Mackain, and E. Clouet, *Acta Mater.*, **78**: 65 (2014).
11. V. O. Kharchenko and D. O. Kharchenko, *Cond. Matter Phys.*, **16**, No. 1: 13801 (2013).
12. V. O. Kharchenko and S. V. Kokhan, *J. Nano- Electron. Phys.*, **7**, No. 2: 012014 (2015).
13. K. R. Elder, M. Katakowski, M. Haataja, and M. Grant, *Phys. Rev. Lett.*, **88**: 245701 (2002).
14. A. Jaatinen, C. V. Achim, K. R. Elder, and T. Ala-Nissila, *Phys. Rev. E*, **80**: 031602 (2009).
15. J. Berry, M. Garnt, and K. R. Elder, *Phys. Rev. E*, **73**: 031609 (2006).
16. D. Kharchenko, V. Kharchenko, and I. Lysenko, *Physica A*, **389**: 3356 (2010).
17. D. Kharchenko, V. Kharchenko, and I. Lysenko, *Cent. Eur. J. Phys.*, **9**, No. 3: 698 (2011).
18. D. O. Kharchenko, V. O. Kharchenko, S. V. Kokhan, and I. O. Lysenko, *Ukr. Fiz. Zhurn.*, **57**, No. 10: 1069 (2012).
19. A. Onuki, *Phase Transition Dynamics* (Cambridge: Cambridge University Press: 2002).
20. A. Minami and A. Onuki, *Phys. Rev. B*, **70**: 184114 (2004).
21. A. Onuki, *Phys. Rev. E*, **68**: 061502 (2003).
22. A. Minami and A. Onuki, *Phys. Rev. B*, **72**: 100101 (2005).
23. D. O. Kharchenko, O. M. Shchokotova, I. O. Lysenko, and V. O. Kharchenko, *Rad. Eff. Def. Sol.*, **170**, Nos. 7–8: 584 (2015).
24. M. Haataja, J. Muller, A. D. Rutenberg, and M. Grant, *Phys. Rev. B*, **65**: 165414 (2002).
25. M. Haataja and F. Leonard, *Phys. Rev. B*, **69**: 081201 (2004).
26. M. Haataja, J. Mahon, N. Provatas, and F. Leonard, *Appl. Phys. Lett.*, **87**: 251901 (2005).
27. D. O. Kharchenko, O. M. Schokotova, A. I. Bashtova, and I. O. Lysenko, *Cond. Matter Phys.*, **18**, No. 2: 23003 (2015).
28. D. O. Kharchenko, V. O. Kharchenko, I. O. Lysenko, and S. V. Kokhan, *Phys. Rev. E*, **82**: 061108 (2010).
29. V. O. Kharchenko and D. O. Kharchenko, *Cond. Matter Phys.*, **14**, No. 2: 23602 (2011).
30. http://lammps.sandia.gov/
31. M. I. Mendelev and G. J. Ackland, *Philos. Mag. Lett.*, **87**: 349 (2007).
32. M. S. Daw and M. I. Baskes, *Phys. Rev. B*, **29**: 6443 (1984).
33. Ch. Kittel, *Introduction to Solid State Physics* (New York: Wiley: 2004).
34. J. D. Honeycutt and H. C. Andersen, *J. Phys. Chem.*, **91**, No. 19: 4950 (1987).
35. D. Faken and H. Jonsson, *Comput. Mater. Sci.*, **2**, No. 2: 279 (1994).
36. A. Stukowski, *Modelling Simul. Mater. Sci. Eng.*, **20**: 045021 (2012).
37. J. H. Li, X. D. Dai, S. H. Liang, K. P. Tai, Y. Kong, and B. X. Liu, *Physics Reports*, **455**: 1 (2008).
38. P. Qing, J. Wei, L. Jie, C. Xiao-Jia, H. Hanchen, G. Fei, and D. Suvranu, *Scientific Reports*, **4**: 5735 (2014).